Frequency Bifurcation Phenomena and Influencing Factors in Wireless Power Transfer Systems: A Comprehensive Investigation

Yanshen Zhao

Shanghai University of Electric Power Department of Electrical Engineering, Shanghai, 200090, China,
yanshenzhao60@gmail.com

Abstract. With the increasing demand for contactless power supply in modern electronic devices and electric vehicles, wireless power transmission (WPT) technology has attracted significant attention as a promising solution. This paper studies the frequency fork and influencing factors in Wireless power transmission (WPT) system. By establishing a mathematical model of the series-compensated transformer, the influence of the coupling coefficient and the secondary-side equivalent resistance on frequency bifurcation was analyzed.The study found that when the coupling coefficient is large or the secondary-side equivalent resistance is small, the system exhibits frequency bifurcation, leading to a decline in transmission efficiency. The theoretical analysis was verified through MATLAB and Simulink simulations. The results show that reducing the coupling coefficient and increasing the secondary-side equivalent resistance can eliminate frequency bifurcation and improve system performance. This paper provides an optimization scheme for the engineering application of wireless power transmission technology, which helps to improve the efficiency and stability of the wireless charging system.

Keywords: Wireless Power Transmission, Frequency Bifurcation, Coupling Coefficient, Efficiency, Secondary Side Equivalent Resistance, Series Compensation

1 Introduction

This document, saved in the “Word 97-2003” format, is a guide to using the Manuscript Template. Before submitting your final paper, check that the format conforms to this guide. In particular, check the text to make ensure that the correct referencing style has been used and that the citations are in numerical order throughout the text. Your manuscript cannot be accepted for publication unless all formatting requirements are met.

Wireless power transmission technology will revolutionize existing charging modes, significantly enhancing the flexibility, convenience, and reliability of equipment and devices such as electric vehicles and smart power systems. It will inject new momentum

J. Iqbal (ed.), *Proceedings of the 2025 2nd International Conference on Mechanics, Electronics Engineering and Automation (ICMEEA 2025)*, Advances in Engineering Research 272,
https://doi.org/10.2991/978-94-6463-821-9_119

into the development of technologies and equipment in fields including electric vehicles, smart grids, medical devices, household appliances, and aerospace. This advancement will better ensure the secure and stable operation of power grids, promote energy interconnection, improve energy utilization efficiency and accessibility, and demonstrate immense market potential. WPT technology was selected as one of the top ten future research directions by the American Technology Review magazine, and the China Association for Science and Technology also included it in the ten Science and technology leading the future [1].

The advantages of magnetically coupled resonant wireless power transfer technology are typically reflected in its high efficiency, long effective transmission distance, adjustable positioning capability, and other beneficial characteristics [2]. Wireless power transmission can generate high-frequency current in the primary-side coil or cable through high-frequency inversion, enabling the secondary-side coil of the separable transformer to receive energy emitted by the primary-side coil via electromagnetic coupling. After energy conditioning, the system meets the power supply requirements of various loads [3]. Wireless power transmission systems separate the power supply and consumption's interfaces, eliminating the need for physical conductors and avoiding contact-induced fires. Unaffected by harsh environmental conditions, they are suitable for energy transfer in flammable or explosive environments and underwater systems. These systems feature high safety, flexible power supply configurations, and reliable technology. In magnetically coupled resonant WPT systems, the frequency splitting phenomenon occurs during power transmission. Specifically, when the coupling coefficient between the transmitter and receiver coils exceeds the critical coupling coefficient, the transmission power reaches a minimum at the natural resonant frequency (determined by the coil inductance and matching capacitance), while achieving maxima at two frequencies deviating from the natural resonant frequency. When maintaining a fixed operating frequency at the natural resonant frequency, the transmission power first increases and then decreases with the growth of the coupling coefficient, reaching its maximum value precisely at the critical coupling coefficient [4]. This phenomenon is called frequency bifurcation. Many researchers have done studies in this field. Han Rucheng pointed out that increasing the primary coil radius and horizontal offset distance can eliminate the frequency splitting phenomenon [5]. Liu Xiaoyang proposed that the saturation characteristics of nonlinear inductors can suppress the generation of frequency splitting in wireless power transfer systems [6]. Han Teng suggested that selecting compensation capacitance values at the boundary between the upper and lower limits of resonant frequency ranges can maintain consistent system efficiency at both high and low bifurcation frequencies [3].

Based on the series-compensated transformer mutual inductance equivalent model and equivalent circuit, this paper analyzes the coupling coefficient of the transformer and the secondary-side equivalent resistance to investigate their relationship with the frequency splitting phenomenon in wireless power transfer. Then analyze the influence of frequency bifurcation on output efficiency.

Finally， based on the above theoretical analysis and combined with the actual model, the mathematical model of the series compensation transformer is built, including the circuit schematic diagram, the mathematical model code, the selection of electrical components, the test results and the verification of the test results. Through matlab and simulink testing, this paper proposed the optimization scheme for the frequency bifurcation phenomenon , which provides an effective basis for the engineering application of radio energy transmission.

2 Theoretical Basis

In inductively coupled energy transfer systems, the loosely coupled transformer exhibits significant leakage inductance in both primary and secondary windings. To reduce voltage and current stress on power switching devices, improve the system power factor, and minimize the apparent power of the supply, it is necessary to incorporate appropriate compensation circuits with capacitors into both the primary and secondary sides of the transformer. After introducing compensation capacitors, the system demonstrates complex high-order characteristics. When the quality factors of the primary and secondary circuits meet specific conditions, multiple resonant frequencies with zero impedance phase angle emerge, leading to the frequency bifurcation phenomenon. So it is of high necessity to conduct analysis on inductively coupled basic circuit topology 、 related physical quantities and capacitive compensation circuit. Based on this， expand the analysis of the causes and conditions of the frequency bifurcation phenomenon.

Using the Series compensation structure transformer to simplify the compute process. Detailed structure is shown in Figure 1. Cp，Rp , ip , Vp , Lp， are respectively the compensation capacitance, resistance, current, high frequency voltage source, and inductance at the transmitting end. Cs，Rs , is , Vs , Ls，Req， are respectively the compensation capacitance, resistance, current, output voltage, inductance, equivalent resistance at the receiving end, and M is the mutual inductance of the primary secondary coil. Among them, the relationship between mutual inductance and self-inductance at both ends is as follows:

$$M = k\sqrt{L_s L_p} \qquad (1)$$

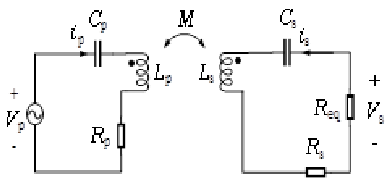

Fig. 1. Series compensation structure transformer (Picture credit: Original)

For the theoretical calculations, the reciprocal equivalence model was used, as shown in Figure 2

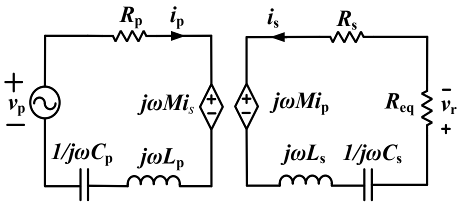

Fig. 2. Mutual inductive equivalence model for the series compensation structure transformer (Picture credit: Original)

When the impedance phase angle equals zero (i.e., the circuit operates at resonance), the following condition holds:

Here，*Z*p is the equivalent impedance of the primary side and *Z*s is the equivalent impedance of the secondary side to the primary side.

$$Z_{in} = Z_p + Z_s \tag{2}$$

$$Z_{in} = R_p + \frac{\omega^2 M^2}{R_s + R_{eq}} \tag{3}$$

Here，*Z*in is the total input impedance when the system is in a resonant state.

For the primary and secondary sides, Kirchhoff's law is used:

$$i_s = \frac{j\omega M V_p}{-\omega^2 M^2 - R_p(R_{eq} + R_s)} \tag{4}$$

$$i_p = \frac{V_p(R_{eq} + R_s)}{\omega^2 M^2 + R_p(R_{eq} + R_s)} \tag{5}$$

$$P_{in} = V_p i_p = \frac{V_p^2(R_{eq} + R_s)}{\omega^2 M^2 + R_p(R_{eq} + R_s)} \tag{6}$$

$$P_{out} = i_s^2 R_{eq} = \frac{V_p^2 \omega^2 M^2 R_{eq}}{\{\omega^2 M^2 + R_p(R_{eq} + R_s)\}^2} \tag{7}$$

$$\eta = \frac{P_{out}}{P_{in}} = \frac{V_p^2 \omega^2 M^2 R_{eq}}{\{V_p^2(R_{eq} + R_s)\}\{\omega^2 M^2 + R_p(R_{eq} + R_s)\}} \tag{8}$$

Here, *P*in and *P*out represent the input power and output power, respectively. And η denotes the transmission efficiency of the transformer. Formula (3) (4) (5) suggest that input power、output power and transmission efficiency are related to multiple parameters of the system. When frequency bifurcation occurs, multiple resonant frequencies emerge, causing associated system performance parameters to bifurcate as well. If the system does not work at the optimal resonant frequency, it cannot guarantee peak performance. By investigating the root causes of frequency bifurcation and its influencing factors, and eliminating the bifurcation phenomenon, the resonant frequency can be maintained at its optimal state. In this paper, the theoretical resonance frequency of the series compensation model was obtained by matlab calculation, and the series compensation model was built by simulink to verify the data of matlab.

3 Project Implementation

3.1 MATLAB data acquisition and analysis

Table 1 shows various parameters of the system

Table 1. System parameter

Parameter	Numerical Value	Parameter	Numerical Value
*L*p/H	49.2*10^-6	*L*s/H	49.2*10^-6
*R*p/Ω	0.2	*R*s/Ω	0.2
*C*p/F	1/(ω^2**L*p)	*C*s/F	1/(ω^2*Ls)
*V*p/V	10	*R*eq/Ω	

(1) When *R*eq=10 Ω

The relationship between the *Z*in *impedance angle* and the *input voltage frequency* of the system is shown in Figure 3

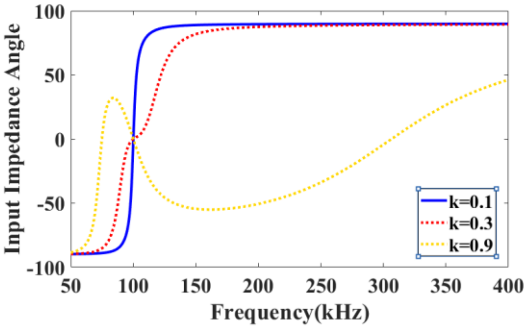

Fig. 3. The relationship between the *Z*in *impedance angle* and the *input voltage frequency* of the system When *R*eq=10Ω (Picture credit: Original)

When the *k* value is 0.1, the *input impedance angle* was mutated around 100 kHz, and remained unchanged after rapidly increasing to nearly 100. Passing a zero point at ω = 100 kHz during this process. When the *k* value is 0.3, with the increase of the frequency, the rise of the *input impedance angle* is fast, then slow, and then fast， totally three stages . It is also maintained at the same angle as when *k* is 0.1. Passing a zero point at ω = 100 kHz during this process. When the *k* value is 0.9, with the increase of the frequency, the *input impedance angle* appears in three stages: "first rise, then decline, then rise". Each stage passes through a zero point, generating a total of three resonant frequencies ω = 75,100,306.5kHz (as shown in Figure 4), and the frequency bifurcation phenomenon occurs.

Fig. 4. Frequency bifurcation point at *R*eq = 10 Ω (Picture credit: Original)

(2) When *R*eq=30 Ω

The relationship between the Zin *impedance angle* and the *input voltage frequency* of the system is shown in Figure 5

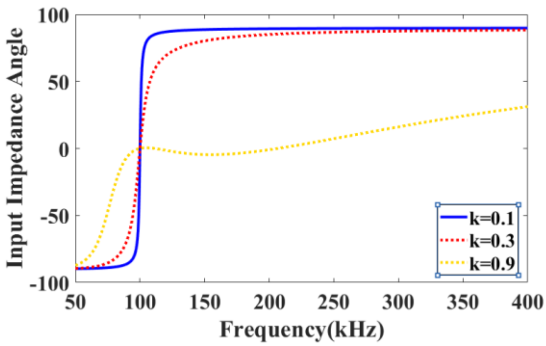

Fig. 5. The relationship between the Zin *impedance angle* and the *input voltage frequency* of the system When *R*eq=30Ω (Picture credit: Original)

When the *k* value is 0.1, the *input impedance angle* was mutated around 100 kHz, and remained unchanged after rapidly increasing to nearly 100. Passing a zero point at ω = 100 kHz during this process.

When the *k* value is 0.3, the *input impedance angle* was mutated around 100 kHz, and remained unchanged after rapidly increasing to nearly 100°. However, the rise rate is slightly slower than the curve when *k* is 0.1. Passing a zero point at ω = 100 kHz during this process. When the *k* value is 0.9, with the increase of the frequency, the *input impedance angle* appears in three stages: "first rise, then decline, then rise". Each stage passes through a zero point, generating a total of three resonant frequencies ω = 75,100,306.5kHz (as shown in Figure 6 and Figure 7), and the frequency bifurcation phenomenon occurs. Comparing Figure 3 with Figure 5， when the value of *k* is the same, the frequency bifurcation occurs in both systems, but the larger *R*eq curve is more flat.

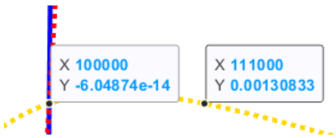

Fig. 6. Frequency bifurcation point at *R*eq = 30 Ω (Picture credit: Original)

Fig. 7. Frequency bifurcation point at *R*eq = 30 Ω (Picture credit: Original)

(3) When *R*eq=50 Ω

The relationship between the *Z*in *impedance angle* and the *input voltage frequency* of the system is shown in Figure 8

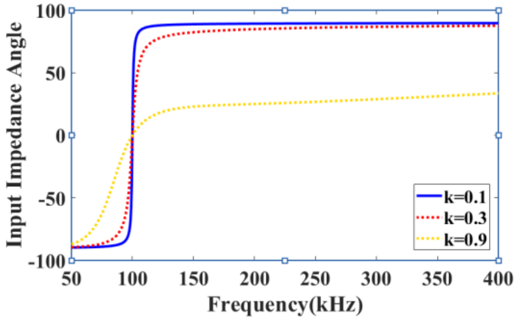

Fig. 8. The relationship between the *Z*in *impedance angle* and the *input voltage frequency* of the system When *R*eq=50Ω (Picture credit: Original)

When the *k* value is 0.1 and 0.3, the *input impedance angle* was mutated around 100 kHz, and remained unchanged after rapidly increasing to nearly 100°. Besides, the higher the *k* value, the slower the *input impedance angle* increases. Passing a zero point at ω = 100 kHz during this process.

When the *k* value is 0.9, as the frequency increases, the *input impedance angle* increases rapidly and then slowly. Passing a zero point at ω = 100 kHz during this process. As shown in Figure 9.Comparing Figure 8 with Figure 5， when the value of *k* is the same, Frequency forks did not occur on the larger side of *R*eq.

According to the above data, it is reasonable to speculate that the frequency bifurcation phenomenon is related to the *k* values and *R*eq values of the system.

Fig. 9. Frequency bifurcation point at *R*eq = 50 Ω (Picture credit: Original)

3.2 Verify the authenticity of data

To further verify the correctness of the matlab data, the simulation model of Figure 1 is constructed in the simulink platform, as shown in Figure10 below:

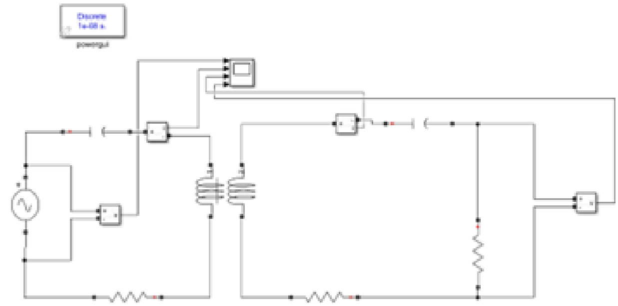

Fig. 10. Simulation model of the series compensation transformer (Picture credit: Original)

1.When *R*eq=10Ω，*ω*=100kHz.Run the model ， the results are shown in Figure 11.If the voltage and current phases of the primary side and the secondary side are identical, the system is operating on the resonance frequency. Due to the presence of multiple resonant frequencies in the system, it is necessary to measure and calculate the detailed parameters under each resonant frequency. Compare these parameters to verify the differential performance of the system at different resonance frequencies.

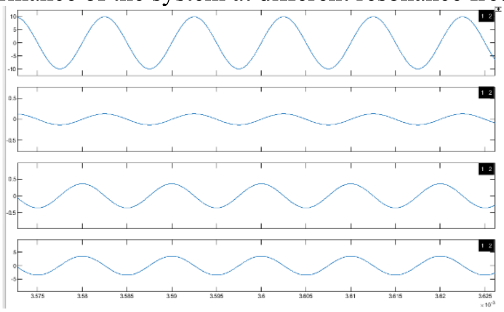

Fig. 11. Voltage and current phase of the system at *ω* = 100 kHz (Picture credit: Original)

Voltage and current of primary side are of same phrase. Voltage and current of secondary side are of same phrase. Measure the voltage and current on the primary and secondary sides. The calculation results show that *P*in=1.313, *P*out=1.28, and the efficiency *η*=97.5%

ω=75kHz.Run the model, the results are shown in Figure 12.

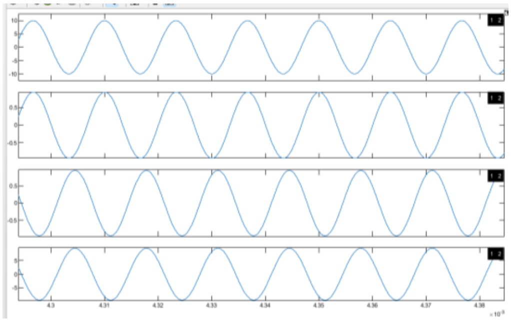

Fig. 12. Voltage and current phase of the system at ω = 75 kHz (Picture credit: Original)

Voltage and current of primary side are of same phrase. Voltage and current of secondary side are of same phrase. Measure the voltage and current on the primary and secondary sides. The calculation results show that *P*in=9.466, *P*out=9.1, and the efficiency η=96.2%, ω=306.5kHz, Run the model， the results are shown in Figure 13.

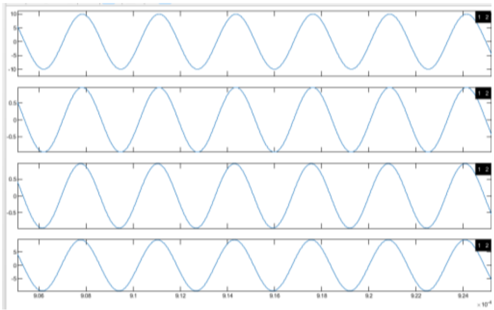

Fig. 13. Voltage and current phase of the system at ω = 306.5 kHz (Picture credit: Original)

The voltage and current of primary side are of same phrase. Voltage and current of secondary side are of same phrase. Measure the voltage and current on the primary and secondary sides. The calculation results show that *P*in=9.607, *P*out=9.2, and the efficiency η=95.8%. When the system operates at different resonant frequencies, the efficiency of power transmission also changes

2.When *R*eq=30Ω,ω=100kHz.Run the model， the results are shown in Figure 14.

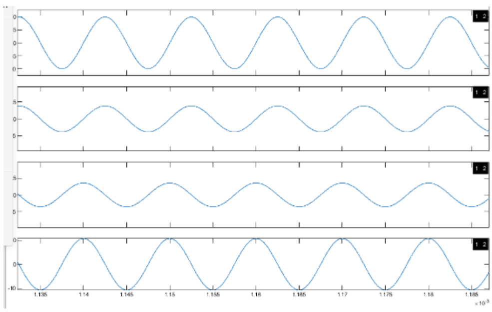

Fig. 14. Voltage and current phase of the system at ω = 100 kHz (Picture credit: Original)

Voltage and current of primary side are of same phrase. Voltage and current of secondary side are of same phrase. Measure the voltage and current on the primary and secondary sides. The calculation results show that *P*in=3.868, *P*out=3.81, and the efficiency η=98.5%

ω=111kHz,Run the model, the results are shown in Figure 15.

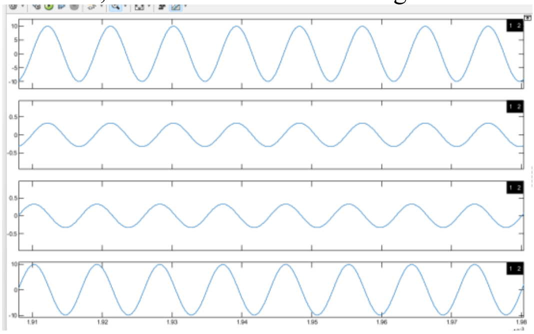

Fig. 15. Voltage and current phase of the system at ω = 111 kHz (Picture credit: Original)

Voltage and current of primary side are of same phrase. Voltage and current of secondary side are of same phrase. Measure the voltage and current on the primary and secondary sides. The calculation results show that *P*in=3.287, *P*out=3.24, and the efficiency η=98.6%

ω=207kHz.Run the model， the results are shown in Figure 16.

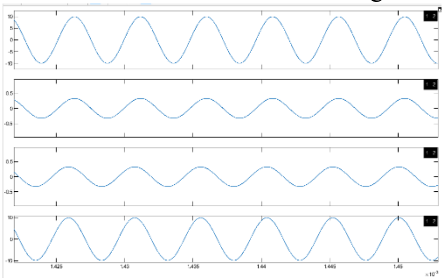

Fig. 16. Voltage and current phase of the system at ω = 207 kHz (Picture credit: Original)

Voltage and current of primary side are of same phrase. Voltage and current of secondary side are of same phrase. Measure the voltage and current on the primary and secondary sides. The calculation results show that *P*in=3.288, *P*out=3.25, and the efficiency η=98.8%

Table 2 is plotted from the calculated data described above

Table 2. The effect of the frequency bifurcation on the system efficiency

*R*eq(Ω) \ω(kHz)	75	100	111	207	306.5

10	96.20%	97.50%	/	/	95.80%
30	/	98.50%	98.60%	98.80%	/

Clearly, the frequency bifurcation phenomenon in the system causes varying operational efficiencies when operating at different resonant frequencies, preventing the system from achieving optimal performance. This negatively impacts the practical application of wireless power transfer, such as reduced wireless charging speed or insufficient power causing devices to fail to maintain operation. This issue is a critical factor that must be eliminated during the product design process.

3.When *R*eq=50Ω

ω=100kHz.Run the model, the results are shown in Figure 17.

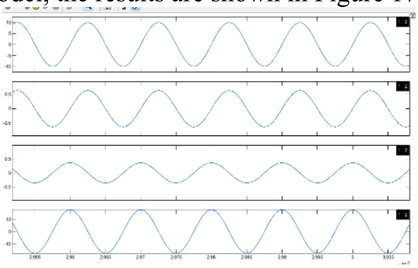

Fig. 17. Voltage and current phase of the system at *ω* = 100 kHz (Picture credit: Original)

Voltage and current of primary side are of same phrase. Voltage and current of secondary side are of same phrase. In conclusion, the data obtained from matlab are correct

It can be seen that the wireless power transmission system may appear more than one resonance frequency point under different working conditions. When the *R*eq value is fixed and the *k* value is large, the system will exhibit a frequency bifurcation phenomenon, and multiple zero-crossing points will appear in the impedance phase angle of *Z*in. When the k value is fixed and the *R*eq value is small, the system will exhibit a frequency bifurcation phenomenon, and multiple zero-crossing points will appear in the impedance phase angle of *Z*in. That is, both the *R*eq and *k* values will influence the frequency bifurcation phenomenon. This paper argues that the frequency bifurcation phenomenon is detrimental to the development and application of wireless power transmission. To prevent the occurrence of frequency bifurcation as much as possible, the system should be operated in under-coupled and critically coupled states while increasing the equivalent resistance on the secondary side. Due to various uncertain factors such as line loss in the actual situation, the actual transmission efficiency will be lower than the data obtained in the simulation experiment, but it can still verify the effect of the secondary equivalent resistance and *k* value on the frequency fork. The experimental results show the feasibility of this scheme.

4 Discussion

Literature [6] points out that the efficiency of the radio energy transmission system is related to the coupling coefficient of the system, and the output power of the system is maximum when the frequency is resonant frequency and the coupling coefficient is 0.1. This paper further verifies this view from the perspective of frequency bifurcation. When the coupling coefficient is low, the system does not have the frequency bifurcation, so the best performance can be achieved. From a practical application perspective, the coupling coefficient of the system can be modified by adjusting coil winding methods to regulate magnetic flux distribution [7][8]. Additionally, this study proposes that the equivalent output resistance on the secondary side also influences the occurrence of frequency bifurcation, though excessive load on the receiver side may simultaneously degrade transmission efficiency [9]. A critical challenge lies in optimizing the equivalent output resistance within a frequency bifurcation-free range while maintaining high transmission efficiency, which remains an open research question. Due to time constraints, this investigation has not explored this trade-off in depth. Notably, practical implementations must also consider additional factors such as cost and economic feasibility, as modifying system parameters often entails significant technical complexity.

Although this paper proposes some optimization schemes in the case of radio energy transmission system, there are many shortcomings and optimization schemes due to the differences between simulation software and practical application, as well as the limitations of the research model. In the selection of system models, this study exclusively adopts the computationally tractable series-series (SS) topology, without considering alternative configurations such as series-parallel (SP), parallel-parallel (PP), or parallel-series (PS) models. The system efficiency also varies under different compensation topology types [10]. Consequently, the derived conclusions exhibit inherent limitations in generalizability , particularly regarding parameter sensitivity and operational stability across diverse circuit architectures. When investigating factors influencing frequency bifurcation, this study primarily focuses on parameters derived from theoretical models, while practical implementations require explicit consideration of coil physical characteristics such as winding turns, cross-sectional area, and spatial configuration, which may significantly alter magnetic coupling dynamics. Furthermore, adjusting the secondary-side equivalent output resistance could be technically achieved through optimization of conductor material resistivity and geometric parameters (e.g., trace length in PCB implementations), though such hardware-level modifications introduce non-negligible trade-offs between impedance matching precision and manufacturing complexity.

5 Conclusion

This paper investigates the frequency bifurcation phenomenon in a series-compensated wireless power transfer system. Through theoretical formula derivation, it is first demonstrated that frequency bifurcation leads to corresponding bifurcation in system performance. MATLAB calculations reveal the relationship between frequency and impedance angle under different parameters, analyzing influencing factors of frequency bifurcation. The study hypothesizes that adjusting the coupling coefficient and secondary-side equivalent resistance can eliminate frequency bifurcation. Then the simulink simulation model is built to verify the conjecture of formula calculation and theoretical calculation. Conclusions indicate that frequency bifurcation reduces system operational efficiency, while decreasing coupling coefficient and increasing secondary-side equivalent resistance can eliminate bifurcation. As wireless power transfer technology finds extensive applications ranging from small electronic devices and medium-power appliances to electric vehicle charging, locomotive power rails, and high-power special scenarios, the research conclusions provide optimization suggestions for enhancing both industrial implementations and daily-life applications of this technology.

References

1. Editorial Department of Science and Technology China: 'Current status and trends of wireless power transmission technology', Sci. Technol. China, 2018, 7, pp. 7–10
2. He, Z.Y.: 'Technical Analysis and Research on Magnetically Coupled Resonant Wireless Power Transfer', Master's thesis, Univ. Electron. Sci. Technol. China, 2019
3. Han, T., Zhuo, F., Yan, J.K., et al.: 'Study on frequency bifurcation phenomena in contactless power transfer systems', Adv. Technol. Electr. Eng. Energy, 2005, 24, (2), pp. 44–47
4. Wang, W.Z.: 'Frequency characteristics of series-parallel systems in magnetically coupled resonant wireless power transmission', Master's thesis, Xi'an Univ. Technol., 2017
5. Han, R.C., Wang, T.M., Zhao, Z.C.: 'Frequency bifurcation phenomena and elimination methods in wireless power transmission systems', Electr. Mach. Control, 2020, 24, (5), pp. 116–123
6. Liu, X.Y., Wang, J.P., Tian, Z.J., et al.: 'Frequency splitting characteristics of nonlinear resonant wireless power transmission systems', Comput. Simul., 2024, 41, (9), pp. 162–166
7. Wang, X.S., Hou, Y.H., Guo, B.C., et al.: 'Research on efficiency influencing factors of magnetically coupled resonant wireless power transmission', Electron. Technol. Softw. Eng., 2022, 20, (3), pp. 121–124
8. Zhu, F., Tang, Y.Y., Ma, H.: 'Impact of coil winding methods on coupling coefficient in inductively coupled power transfer systems', Power Electron., 2015, 10, pp. 16–19
9. Zhang, W.Y., Ma, Y.B., Ou, J.K., et al.: 'Research on influencing factors of wireless power transmission efficiency', Wirel. Internet Technol., 2023, 19, pp. 14–17
10. Zhang, B.K., Deng, J.J., Wang, Z.P., et al.: 'A review of bidirectional wireless power transfer systems for electric vehicles', J. Mech. Eng., 2025, pp. 1–23